

Investigation on Mode – I Fracture Parameters Using Steel Fibers in High Strength Concrete

K. J. Brahma Chari

Department of Civil Engineering, DJR Engineering College, JNTU Kakinada, Vijayawada, Krishna District, A.P, India

Abstract: *Steel fiber high-strength concrete (SFHSC) become in recent decades a very popular material in structural engineering. As a result of increased application of SFHSC, many experimental studies are conducted to investigate its properties and develop new rules for proper design. It has been confirmed by many authors that the specific fracture energy of concrete determined by laboratory experiments depends on the shape and size of the specimen because the local energy in the fracture process zone is influenced by the free surface of the specimen. Mode-I crack propagation in SFHSC is simulated by fracture mechanics. This work aims in studying the mechanical behavior of concrete in terms of modulus of elasticity with the change of aggregate size reinforced with steel fibers of different series for SFHSC concretes. Experiments include compression tests and split tensile strength tests. Study on effect of volume fraction of fibers and change of aggregate size on the modulus of elasticity of concrete was also deemed as an important part of present experimental investigation. The results obtained show that the failure stresses, stress intensity factor, fracture energy and in addition of steel fiber improves the modulus of elasticity of concrete.*

Keywords: Fiber Reinforced Concrete, Size Effect, Stress Intensity Factor, Modulus of Elasticity, Fracture Energy

1. Introduction

Cementitious constituents can be classified into paste, mortar, and concrete categories. ‘paste is defined as the mixture of cement and water, ‘mortar’ is the mixture of small aggregate, such as sand, with paste, and ‘concrete’ is the composite created with larger aggregate, such as gravel or stones, is mixed with mortar. The cement found in these constituents hydrates when mixed with water, forming a hard matrix after curing. While in a liquid form, however, this paste fills the space among aggregates, both large and small, and bonds them together to form mortar or concrete. In addition, a variety of admixtures are used with concrete to improve global behavior, both wet and dry.

During the curing and hardening phases of the hydration process a loss of moisture occurs in the cement paste, causing shrinkage. Shrinkage is the major cause of weak tensile strengths found in concrete, and is also the cause of many internal flaws and cracks that exist in concrete prior to loading. These flaws govern the mechanical behavior of the global concrete material as the flaws initiate and propagate cracks during the application of stresses. Mechanical responses are influenced by the fracture processes of these flaws under loading.

Fibers were used to reinforce brittle materials before cement was known since Egyptian and Babylonian civilizations. It is well known that the main role of fibers is to bridge the cracks that develop in concrete and increase the ductility of concrete elements. Fibers increase the strain at peak load, and provide additional energy absorption ability of RC elements and structures. It was recently reported that they also considerably improve static flexural strength of concrete as well as its impact strength, tensile strength, ductility and flexural toughness.

Fiber reinforcement is usually randomly distributed throughout the whole element, but it can be also used in a part of the element’s section, for example in composite elements like two-layer beams or in high-strength concrete

columns, covered by fiber reinforced concrete. Steel, textile, organic, glass and other kinds of fibers are widely used to improve performance of concrete for about 90 years. For design purposes a very detailed knowledge about the tensile carrying behavior of fibered concrete is required. It is affected by various parameters like fibers’ geometry and content, bond strength between fiber and

binder matrix, strength of the matrix, shrinkage of the concrete orientation of fibers, etc. Effectiveness of fibers added to concrete can be investigated experimentally or numerically. The routine laboratory testing methods are impact test, compressive test, tensile and flexural tests, etc.

The stress- displacement relationship for concrete subjected to uni-axial tension has been divided into four stages based on initiation and propagation of internal cracks and flaws. The first stage includes all loads less than 30% of the peak load; initiation of internal cracks is negligible during this first stage. The second stage spans all loads from the first stage to less than 80% of the peak load. The internal cracks initiate and propagate during this stage; these cracks are generally isolated and randomly distributed. The third stage includes loads over 80% and up to the peak load. At this point micro cracks and flaws begin to link into large, continuous propagating cracks. This phenomenon is known as strain localization. The large crack propagates only when the large load increases, up until the peak load. At this loading point the crack length is referred to as critical crack length. After the peak load is applied major cracks continue to propagate even though the load may decrease.

Since it has been concluded that the fracture behavior of concrete can be characterized by the phenomenon of strain localization, permitting the use of fracture mechanics to describe damage progresses in concrete. The argument stems from the observation that a localized damage band can be physically simulated by a crack; it was therefore concluded that the presence of the strain localization allows the use of fracture mechanics to describe failure of concrete on a microscopic level. Furthermore, since the damage zone of

high-strength concrete is relatively smaller than in normal-strength concrete and the damage band is physically similar to a crack in brittle materials, it was concluded that fracture mechanics is also applicable to high-strength concrete.

1.1 Micro Cracking in Concrete

Concrete is often considered a heterogeneous material in engineering design and construction, yet is in reality a composite consisting of mortar matrix and aggregate inclusion phases. Upon closer inspection, voids are apparent, as the cement paste is actually a mixture of different types of crystalline structures at various degrees of hydration with trapped and entrained air voids. Most researchers simplify concrete as a two-phase composite consisting of mortar and aggregate; to complete the model, defects known as 'micro cracks' are introduced in the system. The failure process is initiated when minute bond cracks form at mortar-aggregate interfaces, while small cracks may also occur in the mortar and aggregate phases separately. Fracture of these micro cracks gives concrete the semblance of ductility; it is the brittle propagation of many micro cracks that form a semi-ductile propagation of a micro crack and ultimately lead to material failure. This fracture process is shown in fig 1.

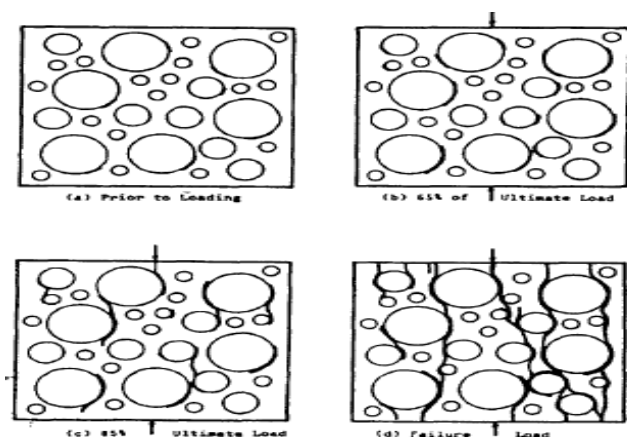


Figure 1: Progressive cracking under uni-axial loading

Fracture mechanics is applied to cracks grown under fatigue loading. Initially the fluctuating load nucleates a crack and grows it slowly but the crack growth rate per cycle picks up speed eventually. A stage is reached when the crack length is long enough to be critical for sudden fracture or catastrophic fracture. Concrete is a quasi-brittle material that exhibits cracking and damage phenomena. It is obvious that economical and safe concrete structures cannot be designed without the use of fracture mechanics. Although in the last two decades significant progress in the field of the application of fracture mechanics in design of concrete and reinforced concrete structures has been made, there are still a number of open questions that need to be solved.

1.2 Modes of Fracture Failure

There are three modes of fracture failure:

- 1) Mode I
- 2) Mode II
- 3) Mode III

Mode I is the opening mode. Mode II is the sliding mode. Mode III causes sliding motion but the displacement is

parallel to the crack front causing tearing (which is also called mixed mode).

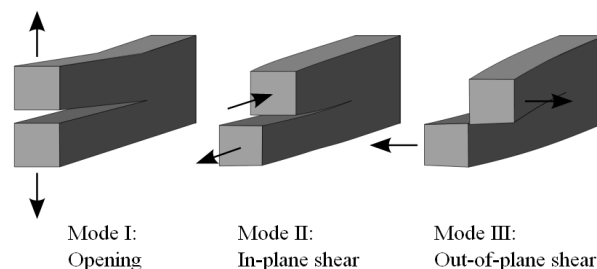


Figure 2: Fracture crack separation modes

Four parameters have been well accepted to measure the potency of a crack.

- 1) Energy release rate (G)
- 2) Stress intensity factor (K)
- 3) J- integral (J)
- 4) Crack tip opening displacement (CTOD)

Energy release rate is energy based and is applied to brittle or less ductile materials. Stress intensity factor is stress based, also developed for brittle or less ductile materials. J- Integral has been developed to deal with ductile material. Its formulation is quite general and can be applied to brittle materials also. Crack tip opening displacement is displacement based which was developed for ductile materials.

At the macro scale level they describe three independent kinematic movements of the upper and lower crack surface with respect to each other and are sufficient to define all possible modes of crack propagation in an elastic material. Of course, at the micro scale the stress distribution is much more complex and at such a level modes of fracture have no sense. As far as concrete is concerned, mode I is a relatively clear type of crack propagation. On the contrary, mode II and III are complex failure modes, which can hardly be realized in an experiment. In these modes the stress normal to the crack surface need to be approximately zero and only in-plane shear stress should exist. Even when these conditions can be realized, due to the complexity of the concrete structure, over a concrete crack surface a combination of different stresses exist (shear, tension, compression and bending). Although the resulting stress may be in-plane stress (shear), complex stress-strain conditions on a crack surface make the identification of mode II and III fracture parameters extremely difficult. Moreover, the question arises whether in a sense of linear elastic fracture mechanics these two failure modes even exist. The similar complex combination of stresses exists for mode I fracture type as well, however, the stress and strain perpendicular to the crack surface dominate at this fracture type.

1.3 Mixed Mode Crack Initiation and Crack Growth

For conservative fracture based design estimates, one needs to characterize the crack under mixed mode loading. In mixed mode condition studies are carried out in finding crack extension direction, critical load and stability of crack path. Various modes have been proposed to characterize the mixed

mode crack. Essentially, the models have been proposed are based either on energy or stresses.

Mixed mode crack propagation criteria:

Following criteria are,

- 1) Modified Griffith criterion
- 2) Maximum tangential stress (MTS) criterion
- 3) Strain energy density (SED) criterion

In the modified Griffith criterion, the concept of energy balance has been extended to include energy release rates associated with all the modes. Total energy release rate for a crack in a plate subjected to mode I and mode II loading is given as, $(G=GI +GII)$. According To This Criterion, crack extension will occur in the direction where the total energy release rate is high and the extension will take place when the maximum energy release rate reaches a critical value. The critical value depends on the material considered. Maximum tangential stress criterion (MTS) was proposed by Erdogan and Sih based on a criterion component of stress state reaching a critical condition.

According to MTS criterion, crack extension will occur in the direction where tangential stress component $\sigma_{\theta\theta}$ at an infinitesimal radial distance r_0 . From the crack tip is maximum and the extension will take place when the maximum tangential stress reaches a critical value which is a materials dependent parameter. Based on energy principles, Sih proposed strain energy density criterion (SED). According to SED criterion, crack extension will occur in the direction of minimum strain energy density $S(\theta)$ and the extension will occur when the $S(\theta)$ reaches a critical value S_c which is a material dependent parameter.

1.4 Crack Growth

For LEFM analysis one of the three criteria, presented above may be chosen for predicting the initiation of the crack extension. In comparison to modified Griffith criterion, MTS criterion and SED criterion are more popular among investigators. Furthermore, MTS criterion is strictly stress based and its analysis does not depend on the condition of plane stress and plane strain. SED criterion deals with strain energy and therefore conditions for predicting crack growth direction and critical applied stress depend on whether the plate is subjected to plane strain or plane stress.

A path of a finite crack growth in a mixed mode case can be predicted by successive application of the fracture criterion. When the given external loading situation reaches the critical stage through a chosen criterion, the existing crack is extended in the predicted critical direction through a small distance. For the newly extended crack configuration we apply the chosen criterion again and criticality of the current loading configuration is checked. If the loading is critical, the crack is extended and the above procedure is repeated. If the condition is subcritical then the crack growth will stop.

2. Research Significance

The main objective of the current study is to review and assess recent experimental results in the field of steel fiber

reinforced high-strength concrete. The research is focused on definition of the main properties of SFHSC that have strong influence on structural behavior. The study explores the hypothesis that the role of fiber reinforcement is to arrest cracking and to keep the crack width low, thereby delaying the age at which visible cracking may be observed.

The present experimental study considers the effect of aggregate size and steel fibers on the modulus of elasticity of concrete. Crimped steel fibers at volume fraction of 0%, 0.5%, 1.0% and 1.5% were used. Study on effect of volume fraction of fibers and change of aggregate size on the modulus of elasticity of concrete was also deemed as an important part of present experimental investigation. The results obtained show that the addition of steel fiber improves the modulus of elasticity of concrete. It was also analyzed that by increasing the fiber volume fraction from 0%, to 1.5% there was a healthy effect on modulus of elasticity of Steel Fiber Reinforced concrete.

3. Material Details

Many researchers have investigated experimentally and theoretically behavior of HSC structures. In most cases the HSC strength was selected based on engineering experience and varied from 60 to 240 MPa.

3.1 Materials

3.1.1 Cement:

Ordinary Portland cement conforming to IS 12269 – 1983 was used for the concrete mix and Specific gravity was found to be 3.5.

3.1.2 Fine Aggregate:

The fine aggregate (sand) used in the work was obtained from a nearby river course. The fine aggregate that falls in zone –II was used. The specific gravity was found to be 2.60.

3.1.3 Course aggregate:

Crushed coarse aggregate of 4.75mm size passing and 10mm retained proportion and 10 mm passing-20mm retained proportion was used in the mix. Uniform properties were to be adopted for all the prisms for entire work. Specific Gravity of coarse aggregate is 2.78.

3.1.4 Admixtures:

To achieve the desired workability CONPLAST SP430 was used as super plasticizer.

3.1.5 Water:

Potable water supplied by the college was used in the work.

3.1.6 Moulds:

Specially made wooden specimens are used for casting prisms. Standard cast iron cube and cylinder were used for casting of cubes, cylinders.

3.1.7 Vibrator:

A device for agitating freshly mixed concrete during placement by mechanical oscillation at a moderately high frequency to assist in consolidation.

3.1.8 Marble Cutter:

The beams were cut with a marble cutter in to the hardened concrete.



Figure 3: Cutting a Beam with Marble Cutter

3.2 Casting:

The moulds were tightly fitted and all the joints were sealed by plaster of Paris in order to prevent leakage of cement slurry through the joints. The inner side of the moulds was thoroughly oiled before going for concreting. The mix proportions were put in miller and thoroughly mixed.

The prepared concrete was placed in the moulds and is compacted using needle & plate vibrators. The same process is adopted for all specimens. After specimens were compacted the top surface is leveled with a trowel.

3.3 Curing:

The NSC specimens were removed from the moulds after 24 hours of casting and HSC specimens were removed after 48 hours of casting, the specimens were placed in water for curing.

4. Test Set Up and Test Procedure

All the specimens were tested on the universal testing Machine of 1000 KN capacity under displacement control at a rate of 0.15mm/min. After 28 days of curing the samples were taken out from the curing tank and kept for dry. After this the sample was coated with white wash. One day later the sample was kept for testing. The beam specimen was kept at the center of testing machine. Beam specimens were put on roller supports exactly under the centre of the load point. For finding the compressive strength of the cube, split tensile strength of the cylinder and the modulus of rupture of the prism specimens were tested on the UTM. The specimen was placed in the machine in such manner that the load was applied on the axis of the specimen was carefully aligned at the center of the loading frame. The load was applied without shock and increased continuously at a constant rate until the resistance of the specimen to the increasing load breaks down and no greater can be sustained. The maximum load applied on the specimen was recorded. A UTM was computerized which was used to measure the deflections under the mid span below the load point.

Table 1: Quantities of Materials

Grade	Proportions	Cement Kg/m ³	F.A Kg/m ³	C.A Kg/m ³	Water %	S.P ML/kg
M25	1:1.142:2.56	443.322	506.273	1134.90	0.43	-
M50	1:1.472:3.043	409.207	602.352	1245.216	0.35	37
M75	1:1.2:2	542.98	651.570	1085.96	0.22	37



Figure 4: Test Setup

5. Results and Discussions

The beam specimens were tested on the Universal Testing Machine under displacement rate control. All the beam specimens were tested under the three points bending under the displacement rate control. A photograph of the test setup is shown in Fig 4.0. To understand the fracture behavior of plain concrete beams the following graphs were drawn, Load Vs Mid span deflection (Fig 5.0, 5.1, 5.2). The normal and shear stress and stress intensity factor and fracture energy of the beams subjected to three point bending with eccentric notch calculated by using the eq.s (5.1 to 5.8) and reported in Table 5.0 and in table 5.1. From the graphs and Tables it was observed that, for mixed-mode failure of concrete, It was found that the stress intensity factor and fracture energy increases with the increasing of beam sizes and decreasing the failure stresses with increasing the beam sizes. The brittleness of the beam increases with increase the size of the beam.

Based on the tests on Concrete beams it can be observed that, in the case of eccentric notched plain concrete beams, the first crack appeared in the tension zone at notch tip. The deflections were measured only up to the ultimate load and failed suddenly in to two pieces.

5.1 Calculations

$$\sigma_n = 6M / (bt^2 (1-\alpha)) \quad 5.1$$

$$\tau_n = V / (bt (1-\alpha)) \quad 5.2$$

$$M = \{ (p/4) (s-2x) \} + \{ (wl/4) (s-2x) \} - \{ (w/8) (1-2x) \}^2 \quad 5.3$$

$$V = \{ (p/2) + (wx) \} \quad 5.4$$

$$K_I = \sigma_n * \sqrt{b} * \sqrt{(\prod^* \alpha)} * f_{I1}(\alpha) \quad 5.5$$

$$K_{II} = \tau_n * \sqrt{b} * \sqrt{(\prod^* \alpha)} * f_{II1}(\alpha) \quad 5.6$$

$$f_{I1}(\alpha) = 0.689$$

$$f_{II1}(\alpha) = 0.53$$

$$K = \sqrt{(K_I^2 + K_{II}^2)} \quad 5.7$$

$$G = K^2 / E \quad 5.8$$

σ_n = normal stress, τ_n = shear stress, M = bending moment at distance x, V = shear force at distance x, w = wt. per unit length of the beam, p = point load, α = a/b (notch depth to beam depth), s = nominal span, l = length, b = depth, t = thickness, $f_{I1}(\alpha)$ and $f_{II1}(\alpha)$ are dimensionless parameters, K_I = stress intensity factor of mode I, K_{II} = stress intensity factor of mode II, K = stress intensity factor for mixed mode, G = fracture energy for mixed mode, E = young's modulus.

Table 2: Failure stresses (normal and shear stress)

Specimen designation	Ultimate Load KN	Normal stress(σ) n/mm ²	Shear stress (τ) n/mm ²
S-25	06.000	7.447	0.667
M-25	10.150	6.384	.0565
L-25	16.500	6.181	0.461
S-50	6.450	8.037	0.717
M-50	11.150	7.009	0.620
L-50	18.500	6.910	0.516
S-75	06.150	7.660	0.683
M-75	11.000	6.910	0.612
L75	17.000	6.360	0.475

Table 3: stress intensity factors and fracture energy

Specimen designation	Ultimate Load KN	Stress intensity factor (n/mm ²)m ²	Fracture energy n/mm
S-25	06.000	1.120	0.044
M-25	10.150	1.353	0.064
L-25	16.500	1.851	0.120
S-50	06.450	1.204	0.036
M-50	11.150	1.485	0.054
L-50	18.500	2.070	0.106
S-75	06.150	1.148	0.026
M-75	11.000	1.465	0.043
L-75	17.000	1.906	0.073

Fracture energy for non linear was calculated from formula,

$$G = \frac{U - 0.5mg\delta_0}{1.15bh \left[1 - \frac{a_0}{h} \right] / \cos \alpha}$$

Where, U is the area under the load versus vertical deflection curve up to the point of instability

δ_0 is the vertical deflection at the instability point.

α is the angle between the vertical plane and the crack plane

(a_0/h) is the notch depth ratio.

$Mg = w =$ unit weight of the beam

Table 4: Fracture Energy for non linear from Formula

Specimen designation	Ultimate load KN	Fracture energy (G Formula) n/mm
S-M25	06.000	0.049
M-M25	10.150	0.062
L-M25	16.500	0.052
S-M50	06.450	0.109
M-M50	11.150	0.160
L-M50	18.500	0.113
S-M75	06.150	0.066
M-M75	11.000	0.069
L-M75	17.000	0.074

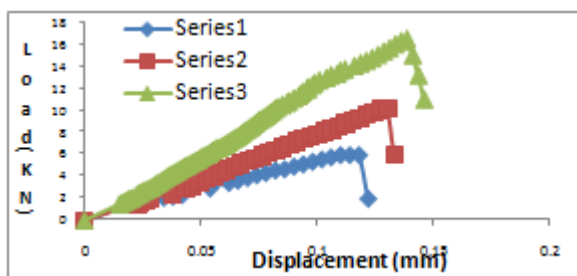


Figure 5: Load-Displacement diagrams for M25-Small, Medium, and Large beams

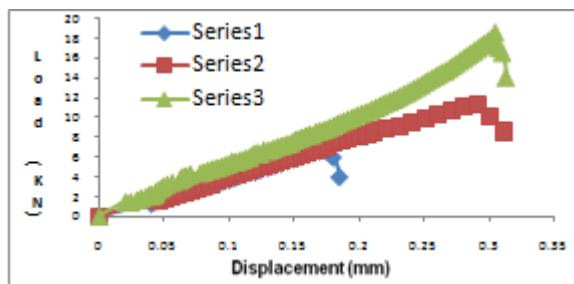


Figure 6: Load-Displacement diagrams for M50-Small, Medium, and Large beams

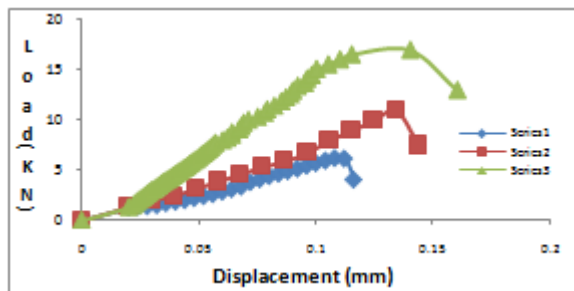


Figure 7: Load-Displacement diagrams for M75-Small, Medium, and Large beams

6. Analytical Work

ANSYS SOFTWARE: - ANSYS is a general purpose finite element modeling package for numerically solving a wide variety of mechanical problems. These problems include: static/dynamic structural analysis (both linear and non-linear), heat transfer and fluid problems, as well as acoustic and electromagnetic problems.

6.1 Solution of Finite Element Problem by using ANSYS

In general, a finite element solution may be broken into the following three stages. This is a general guideline that can be used for setting up any finite element analysis.

- 6.1.1) Preprocessing
- 6.1.2) Solution
- 6.1.3) Post processing

6.1.1) Preprocessing: - Defining the problem involves the major steps like

- Define key points/lines/areas/volumes
- Define element type and material/geometric properties
- Mesh lines/areas/volumes as required
- Dimensionality of the analysis (i.e. 1D, 2D, axi-symmetric, 3D).

6.1.2) Solution

- Assigning loads: here we specify the loads (point or pressure)
- Constraints: here we specify constraints (translational and rotational)
- Solving: finally solve the resulting set of equations.

6.1.3) Post processing: - in this stage we can see

- Lists of nodal displacements

- Element forces and moments
- Deflection plots
- Stress contour diagrams

Table 5: Comparison of failure stresses (normal and shear stress) from manual and ANSYS

Sizes	UL Kn	Experimental normal stress (n/mm ²)	Ansys normal stress(n/mm ²)	Ratio (σ_e/σ_a)
S-M25	6.000	7.445	6.615	1.125
M-M25	10.150	8.037	7.565	1.062
L-M25	16.500	7.660	8.511	0.900
S-M50	6.450	6.384	4.810	1.327
M-M50	11.150	7.009	5.284	1.326
L-M50	18.500	6.910	5.213	1.325
S-M75	6.150	6.181	7.464	0.828
M-M75	11.000	6.910	8.369	0.825
L-M75	17.000	6.360	7.691	0.826

Table 6: Comparison of failure stresses (normal and shear stress) from manual and ansys

Sizes	UL Kn	Experimental Shear Stress (n/mm ²)	Ansys Normal Stress (n/mm ²)	Ratio (τ_e/τ_a)
S-M25	6.000	0.667	0.540	1.235
M-M25	10.150	0.717	0.658	1.089
L-M25	16.500	0.683	0.637	1.072
S-M50	6.450	0.565	0.464	1.217
M-M50	11.150	0.620	0.510	1.215
L-M50	18.500	0.612	0.503	1.216
S-M75	6.150	0.416	0.500	0.832
M-M75	11.000	0.516	0.561	0.919
L-M75	17.000	0.475	0.515	0.922

UL = ultimate load,

σ_e = Experimental normal stress,

σ_a = Ansys normal stress,

τ_e = Experimental shear stress

τ_a = Ansys normal stress

It is observed that the ratio between normal stress from experimental and Ansys varies from 0.900 to 1.125 for M25 grade concrete, 1.325 to 1.327 for M50 grade concrete and 0.825 to 0.828 for M75 grade concrete and also observed that the ratio between shear stress from experimental and Ansys varies from 1.072 to 1.235 for M25 grade concrete, 1.215 to 1.217 for M50 grade concrete and 0.832 to 0.922 for M75 grade concrete.

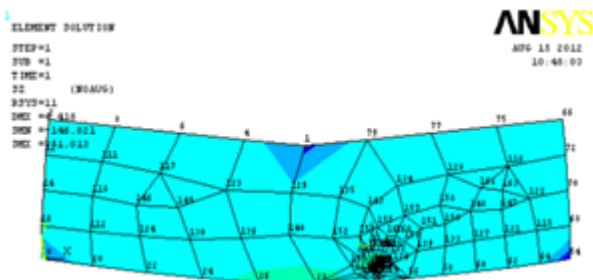


Figure 8: Stress Intensity in the Beam in Ansys

7. Conclusion

Based on the tests on twenty seven notched concrete beam specimens, the following conclusions have been drawn:

1. It is observed that, failure stresses (normal stresses and shear stresses) decreases with increasing of beam sizes.
2. It is also observed that, stress intensity factor increases with increasing in beam sizes for all grades of concrete.
3. It is also observed that, fracture energy increases with increasing in beam sizes for all beams.
4. It is also notice that, the larger the beam, the more leaned towards the load point the crack trajectory was.

8. Future Developments of SFRHSC

SFHSC has passed from a new material to one that became successful and widely applied because of its mechanical properties and advantages over the conventional concrete. The current review has tended to emphasize various aspects of SFHSC usage. However it would not be complete without mentioning the problems and limitations, associated with the material. Most of the problems are associated with producing the SFHSC mix (mixing, handling, bailing problem, etc.) And it's casting. However, it is possible to overcome these problems by using modern technologies and equipment. For example, devices, dispensing fibers automatically, are used to limit balling.

In the hardened state, fibers pose a few additional problems. One of them is that steel fibers corrode if cracking occurs. Corrosion decreases the positive effect of fibers. A question how long steel fibers will last under specific conditions is still important. The problem is positively addressed by the development of fibers offering corrosion resistance by their chemical composition. Finding alternative ways is one of the directions for further applications of SFHSC.

Concrete mix properties, yielding best fibers' location and most effective action in hardened SFHSC, can be successfully predicted at the design stage. The idea of two-layer beams, in which SFHSC was proposed to be used just in the compressed zone, is aimed at decreasing the fiber content and consequently the cost of the bending element. Understanding that stresses are not uniformly distributed along the compressed zone, it is more logically to have higher fiber content at the part of the compressed zone, where higher stresses appear. However, even modern techniques don't enable to change the fiber amount during the casting process. Therefore, today the fiber content is determined by the maximum tensile stress in concrete members, resulting in relatively high fiber expenditure. Developing appropriate techniques for control and varying the fiber content during casting of SFHSC elements would allow more effective fiber placement and lower cost of SFHSC elements. If the optimal amount of fibers could be regulated during casting, a further step for improving the performance of SFHSC could be more accurate design of structural elements using modern finite elements software allowing taking into account variations in real materials properties, various load cases and considering available data for proper design. The calculation results could be transmitted to a concrete casting system for addition of a required optimal fibers' content at each layer.

Using nondestructive techniques in real time during casting would allow obtaining a feedback for online prediction of hardened SFHSC properties. For this reason neural networks and modern system identification techniques may be also employed. Using mathematical models, applied for

experiments' planning could enable to correct the fiber content online based on the predicted SFHSC properties.

Acknowledgment

The author is wishing to thank Dr. V.Ranga Rao & Mr. P. Siva Sankar for guidance and stimulation.

References

- [1] Nawy EG. Fundamentals of high strength high performance concrete. Harlow, Essex, England: Longman group limited; 1996.
- [2] Mohammadi Y, Singh SP, Kaushik SK. Properties of steel fibrous concrete containing mixed fibres in fresh and hardened state. *Constr Build Mater* 2008; 22:956–65.
- [3] Iskhakov I, Ribakov Y. A design method for two-layer beams consisting of normal fibered high strength concrete. *Mater Des* 2007; 28(5):1672–7.
- [4] Hadi MNS. Reinforcing concrete columns with steel fibres. *Asian J Civil Eng* 2009; 10(1):79–95.
- [5] Gani MSJ. Cement and concrete. London: Chapman & Hall; 1997.
- [6] Heinzle G, Freytag B, Linder J. Rissbildung von biegebeanspruchten Bauteilen aus Ultrahochfestem Faserbeton. *Beton und Stahlbetonbau* 2009; 104(9):570–80.
- [7] Wang ZL, Wu J, Wang JG. Experimental and numerical analysis on effect of fibre aspect ratio on mechanical properties of SRFC. *Constr Build Mater* 2010; 24:559–65.
- [8] M.T. Kazemi and I. Zakeri (2009) “investigation into the mixed mode fracture of steel fiber reinforced concrete (SFRC) beams with one percent volume fraction of steel fiber”
- [9] Gonzalo Ruiz ha (2007) “Mixed-mode crack propagation through reinforced concrete.”+
- [10] Parviz Soroushian, Hafez Elyamany, Atef Tlili and Ken Ostowari (1998) “Mixed mode Fracture properties of Concrete Reinforced with low volume fractions of steel and Polypropylene Fibers” *Cement and Concrete Composites* 20, 67-78.
- [11] Swartz, S.E., Lu, L.W. and Tang L.D (1998) “Mixed mode fracture toughness testing of concrete beams in three point bending” *Mater. Struct.* 21, 33-40.
- [12] Jan G. Rots and Ren de Borst (1987) “analysis of mixed-mode fracture in concrete.”
- [13] Luigi Biolzi (1990) “ mixed mode fracture in concrete beams; mixed mode experiments over symmetrically notched beams of concrete”
- [14] P. Bocca (1990) “Size effects in the mixed mode crack propagation”
- [15] S.E.Swartz, N.M.Taha(1990)“Mixedmode crack propagation and fracture in concrete”
- [16] 1991 A.K. Maji (1991) “ mixed mode crack propagation in quasi-brittle materials”
- [17] B. Shen (1993) “ Numerical analysis of mixed mode I and Mode II fractures propagation”
- [18] V. O. García-Álvarez (1994) “ an analysis of mixed mode fracture in quasi-brittle materials using the discrete crack method”
- [19] B. M. Liaw, N. M. Hawkins (1998) “fracture-process zone for mixed-mode loading of concrete”
- [20] Parviz Soroushian(1998) “Mixed-mode fracture properties of concrete reinforced with low volume fractions of steel and polypropylene fibers”
- [21] J.M. Chandra Kishen (1998) “mixed mode fracture of cementitious bimaterial interfaces”
- [22] J. Özbolt and H.W. Reinhardt(2000) “numerical study of mixed-mode fracture in concrete”
- [23] Pendyala R, Mendis PA, Patnaikuni I. Full range behavior of high-strength reinforced concrete flexural concrete members. *ACI Struct J* 1996; 93. 1.
- [24] Mansur MA, Chain MS, Wee TH. Flexural behavior of high strength concrete beams. *ACI Struct J* 1997; 94(6).
- [25] Magnusson J, Hallgern M. Reinforced high strength concrete beams subjected to air blast loading. In Jones N, Brebbia CA, editors. *Structures under shock and impact VIII*. WIT Press; 2004.
- [26] Ramadan OMO, Kansouh SF. an empirical model for curvature ductility of reinforced high-strength concrete sections. In *Proceedings of the seventh international conference on computational structures technology*. Paper No.176. Lisbon: Civil-Comp Press; 2004.
- [27] Shah SA, Ribakov Y. Experimental and analytical study of flat-plate floor confinement. *Mater Des* 2005;26(8):655–69.
- [28] J.C. Gálvez (2002) “a discrete crack approach to normal/shear cracking of concrete”
- [29] Yangjian Xu (2011) “an Applications of normal stress dominated cohesive zone models for mixed-mode crack simulation based on extended finite element methods”
- [30] T.D.Gunneswararao, Ch.N.Satish Kumar (2008) “investigation on fracture behavior of steel fiber reinforced concrete beams subjected to three point bending”
- [31] Luciani N. Lens(2009) “Constitutive models for cohesive zones in mixed-mode fracture of plain concrete”

Author Profile



Mr. K. J. Brahma Chari is currently pursuing master's degree program in Structural Engineering, Department of Civil Engineering, DJR Engineering College, Jawaharlal Nehru Technological University Kakinada, Vijayawada, Krishna District, Andhra Pradesh, India



Dr. V.Ranga Rao, Dean of Research and consultancy, Department of civil engineering, KL University, Vaddeswaram, Guntur, Andhra Pradesh, India